

# Thermally programmed one-pot CRISPR assay for on-site pandemic surveillance

Received: 17 June 2025

Accepted: 9 October 2025

Published online: 21 November 2025

 Check for updates

Zhen Huang<sup>1,2,14</sup>, Yajuan Dong<sup>3,4,14</sup>, Yang Yang<sup>5,14</sup>, Xuchun Han<sup>6,14</sup>, Fuxiang Wang<sup>5</sup>, Christopher J. Lyon<sup>1,7</sup>, Shuai Ding<sup>6</sup>, Yun Peng<sup>5</sup>, Ganggang Zhang<sup>8</sup>, Christina Hu<sup>1,9</sup>, Huan Huang<sup>4</sup>, Liu Yang<sup>5</sup>, Guoping Zhao<sup>10</sup>, Xiao-Yong Fan<sup>3</sup>✉, Shuihua Lu<sup>4,5</sup>✉, Tony Hu<sup>1,7,11</sup>✉ & Jin Wang<sup>6,12,13</sup>✉

The ongoing monkeypox virus outbreak highlights the need for rapid and accurate diagnostics to enhance epidemic control. CRISPR-based assays hold promise, but clinical translation is hindered by high complexity and low throughput. Here, we describe a thermally regulated asynchronous CRISPR-enhanced (TRACE) assay that rapidly and sensitively detects multiple DNA targets in a streamlined, one-pot format. TRACE exhibits a 2.5 copies/test limit of detection – 40 times lower than a canonical one-pot CRISPR. When applied to clinical samples, it achieves 99.5% accuracy across diverse sample types, and can detect MPXV within 11 minutes. Point-of-care TRACE assays meet ASSURED criteria and deliver comparable performance to qPCR, with a fivefold reduced report time, in outpatient settings. Moreover, TRACE enables simultaneous detection of pathogen and host genes at comparable sensitivity to address a critical limitation of current CRISPR assays, which lack internal controls. TRACE thus enables rapid, on-site surveillance to facilitate bench-to-bedside translation of CRISPR diagnostics.

Increasing interactions between human and non-domesticated populations render it a question of a “when” rather than “if” the next pandemic caused by an emerging disease will occur<sup>1</sup>. Monkeypox virus (MPXV) serves as another recent example of a zoonotic pathogen that has spilled over into human populations and established sustained human-to-human transmission<sup>2</sup>. There have been two major international MPXV outbreaks that resulted in ~120,000 reported MPXV cases and 300 deaths worldwide<sup>3</sup>. Newly emerging strains and the potential for further mutations, particularly those that enhance aerosol transmission, indicate the risk for future pandemics<sup>4–6</sup>. Recent pandemics

underscore the critical importance of early identification and containment in mitigating disease transmission<sup>7</sup>, and the need for widely accessible, easy-to-use, and highly effective diagnostic tools<sup>8</sup>.

New CRISPR-based diagnostic platforms are positioned leading candidates to address future infectious disease outbreaks<sup>9,10</sup>. Under optimal conditions, these platforms can detect nucleic acid targets at single-molecule resolution and distinguish targets differing by single-nucleotide polymorphisms to provide exceptional diagnostic accuracy<sup>11–13</sup>. CRISPR diagnostics are modular in design and can be rapidly reconfigured to detect a different pathogen by replacing their

<sup>1</sup>Center for Cellular and Molecular Diagnostics, Tulane University School of Medicine, New Orleans, LA, USA. <sup>2</sup>Department of Medicine, Tulane University School of Medicine, New Orleans, LA, USA. <sup>3</sup>Shanghai Public Health Clinical Center & Shanghai Institute of Infectious Diseases and Biosecurity, Fudan University, Shanghai, China. <sup>4</sup>National Clinical Research Center for Infectious Diseases, Shenzhen, China. <sup>5</sup>Shenzhen Third People's Hospital, Southern University of Science and Technology, Shenzhen, China. <sup>6</sup>Wuxi Tolo Biotechnology Co., Ltd., Wuxi, China. <sup>7</sup>Department of Biochemistry and Molecular Biology, Tulane University School of Medicine, New Orleans, USA. <sup>8</sup>Institute of Microbiology, Jiangxi Academy of Sciences, Nanchang, China. <sup>9</sup>Phillips Exeter Academy, Exeter, NH, USA. <sup>10</sup>Key Laboratory of Systems Health Science of Zhejiang Province, School of Life Science, Hangzhou Institute for Advanced Study, University of Chinese Academy of Sciences, Hangzhou, China. <sup>11</sup>School of Biomedical Engineering, Tsinghua University, Beijing, China. <sup>12</sup>Shanghai Tolo Biotechnology Co., Ltd., Shanghai, China. <sup>13</sup>School of Life Sciences, Huaibei Normal University, Huaibei, China. <sup>14</sup>These authors contributed equally: Zhen Huang, Yajuan Dong, Yang Yang, Xuchun Han. ✉e-mail: [xyfan008@fudan.edu.cn](mailto:xyfan008@fudan.edu.cn); [lushuihua66@126.com](mailto:lushuihua66@126.com); [tonyhu@tulane.edu](mailto:tonyhu@tulane.edu); [wangjin@tolobio.com](mailto:wangjin@tolobio.com)

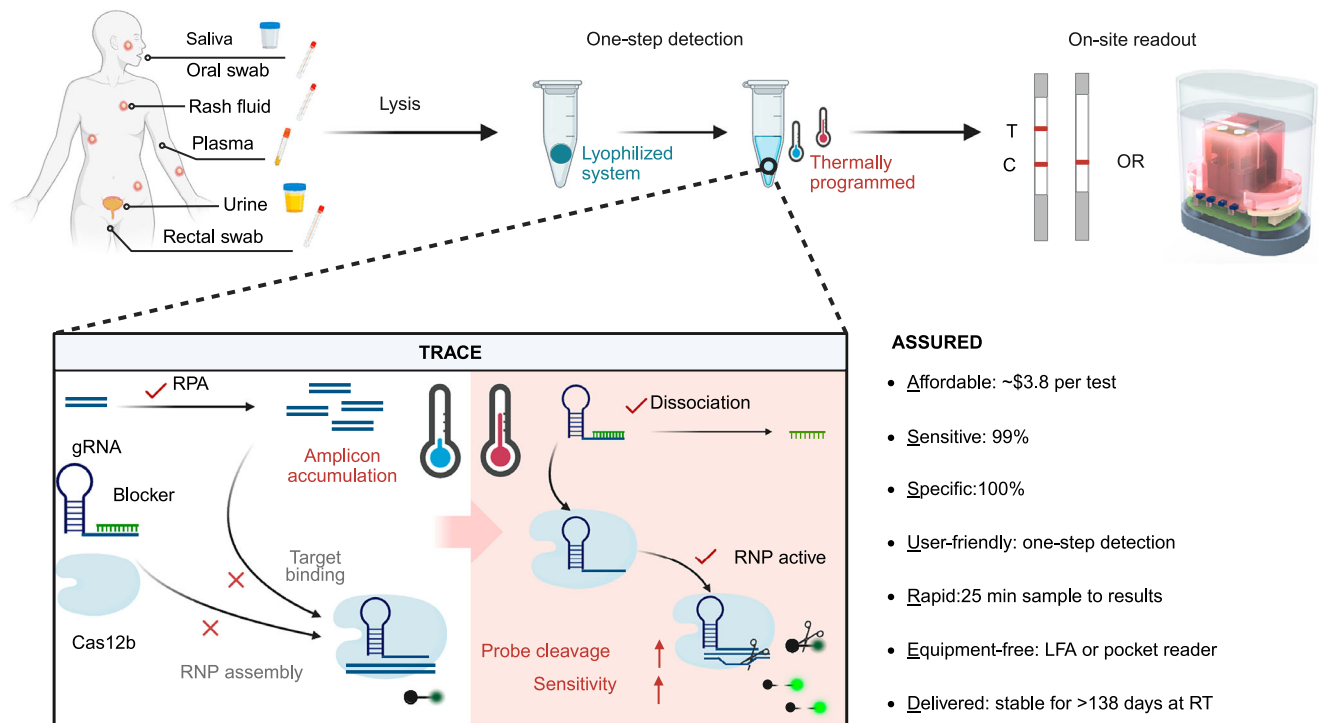


**Fig. 1 | TRACE assay design.** Created in BioRender. Dong, Y. (<https://BioRender.com/uhs299y>). In the one-pot TRACE assay workflow, lysed clinical samples are directly added to lyophilized TRACE reagents, and subjected to a two-stage incubation procedure employing asynchronous recombinase polymerase amplification (RPA) and CRISPR/Cas12b reactions for sensitive target detection, and visualizing assay results for point-of-care testing with lateral flow assay strips or a portable device. TRACE employs differences in the optimum temperatures for RPA and Cas12b activity and the annealing of a single-stranded RNA (ssRNA) blocker with gRNA to segregate RPA and Cas12b activity. Cas12b:gRNA ribonucleoprotein

complex assembly and target cleavage is suppressed during the low-temperature stage by ssRNA blocker and temperature effects, allowing efficient accumulation of the target amplicon. Conversely, RPA is inactivated and Cas12b is reactivated in the high-temperature stage by gRNA:ssRNA dissociation and Cas12b RNP formation, leading to efficient target recognition/cleavage and probe degradation to maximize assay sensitivity. Lateral flow TRACE assays can also fulfill ASSURED (affordable, sensitive, specific, user-friendly, rapid, equipment-free, and delivered) criteria for point-of-care tests.

guide RNA (gRNA)<sup>10</sup>, a key advantage for a swift response to an emerging infectious disease outbreak. However, despite their promise, the bench to bedside transition of CRISPR diagnostics remains an ongoing challenge, partly due to the serial nature of most CRISPR diagnostic workflows and partly due to the difficulty of generating multiplex assays<sup>9</sup>.

Conventional CRISPR diagnostics employ a two-step approach, where the nucleic acid amplification (NAA) and CRISPR detection reactions are performed in series, but this increases assay complexity and the risk for cross-contamination<sup>11–13</sup>. Several strategies have been investigated to integrate these reactions into streamlined protocols. A single-tube assay immobilized CRISPR reagents above the NAA reaction, introducing them to completed NAA reactions in closed tubes by centrifugation<sup>14,15</sup>, to avoid aerosol transfer after NAA completion and sensitivity losses from competition between the NAA and cleavage reactions. However, this approach risks prematurely dislodging the affixed CRISPR reagents during tube manufacture, storage, or handling<sup>9</sup>. A second, more common one-pot assay strategy employs isothermal conditions compatible with simultaneous NAA and CRISPR reactions<sup>16,17</sup>. One widely adopted design integrates the CRISPR reaction with recombinase polymerase amplification (RPA), which shares a highly overlapping temperature range and a compatible buffer system with CRISPR<sup>17–19</sup>. However, this approach requires careful optimization since its CRISPR activity can deplete the shared amplicon target of these reactions to reduce NAA efficiency, leading to inferior assay performance<sup>18,19</sup>, which can be worse than qPCR<sup>17</sup>. Recent studies have sought to address this challenge by using gRNAs with suboptimal or missing protospacer adjacent motif recognition sequences to reduce CRISPR efficiency<sup>18,19</sup> and balance NAA and CRISPR reaction activity,

but this gRNA screening process is labor-intensive and resulting assays still typically exhibit lower sensitivity than two-step assays. Modified gRNAs with photodegradable molecular locks that block Cas12a/gRNA target recognition and cleavage have also been tested for their ability to reduce interference with the NAA reaction<sup>20</sup>. However, while this approach can improve overall performance, it also increases assay complexity, cost, and completion time.

Multiplex detection also remains a major challenge<sup>9</sup> since conventional CRISPR-based assays employ the low specificity trans-cleavage activity of their CRISPR associated protein (Cas) to unmask the fluorescence of quenched reporters<sup>11–13</sup>. Multiplex assays developed using Cas variants with selective trans-cleavage specificities have attempted to address this issue, but remain subject to off-target cleavage activity that impairs target resolution and assay interpretation<sup>21</sup>. Several methods have also been used to partition distinct assays into distinct chambers on a chip to allow parallel detection of multiple targets<sup>22,23</sup>, but these approaches are hindered by high costs and the need for specialized readout equipment, limiting their utility for diagnostic applications.

Here, we present a thermally regulated asynchronous CRISPR-enhanced (TRACE) one-pot duplex assay platform (Fig. 1) that employs the temperature profiles of RPA, Cas effectors, and a ssRNA gRNA inhibitor to thermally segregate NAA and CRISPR activity to enhance the detection of low abundance targets. Single-plex TRACE detects 2.5 MPXV target copies/test, matching the sensitivity of standard two-step CRISPR methods, while a lateral flow TRACE assay, which does not require nucleic acid isolation, refrigeration, or expensive equipment and meets REASSURED criteria, demonstrates performance that is comparable to qPCR for numerous clinical sample types, despite being

faster and less expensive. A third TRACE variant, which employs an integrated RPA/Cas12a reaction to allow duplex detection of a host gene as an internal control for sample quality, addresses a key concern for clinical translation. These TRACE assay formats could thus facilitate disease screening efforts at testing sites with variable resource levels, including resource-limited settings.

## Results

### TRACE assay design and characterization

An in-silico analysis of MPXV genome sequences available in the NCBI database revealed that RPA primer and gRNA sequences complementary to a conserved region within the MPXV *J2L* gene provided broad coverage (99.6%) of reported MPXV strains with complete specificity (Supplementary Fig. 1a-d, Supplementary Data 1-2, and Supplementary Tables 1-2). A two-step Cas12a assay generated with these primer and gRNA sequences revealed high sensitivity (2.5 copies/test) and specificity (Fig. 2a and Supplementary Fig. 2, and Supplementary Table 3). However, an optimized one-pot Cas 12a assay generated from this assay revealed substantially reduced sensitivity (100 copies/test) due to a Cas12a-mediated inhibition of the RPA amplification reaction (Fig. 2b), which could impair target detection in patient samples with low viral loads, including urine and specimens from individuals with early-stage infections, to limit overall diagnostic performance<sup>24</sup>.

We therefore replaced Cas12a with Cas12b, which has comparable cis- and trans-cleavage activity but a broader reported temperature range (31–59 °C)<sup>25</sup>, attempting to leverage the moderate difference in the RPA and Cas12b temperature optimums to segregate their activities in a one-pot assay to enhance its sensitivity. We found that an optimized one-pot RPA/Cas12b assay employing sequential 37 °C and 60 °C incubations revealed improved sensitivity (10 copies/test) due to attenuated Cas12b-mediated amplicon cleavage, validating our hypothesis, although weak reporter signal detected at the end of the first stage revealed the presence of residual Cas12b activity (Fig. 2c).

Based on previous gRNA engineering studies<sup>20</sup>, we next evaluated whether single-stranded RNAs (ssRNAs) complementary to the gRNA spacer region could attenuate this residual Cas12b cleavage activity during the 37 °C amplification phase. We detected substantial reductions in both cis- and trans-cleavage activity during this interval, resulting in improved assay sensitivity (2.5 copies/test) comparable to the two-pot RPA/Cas12a assay, due to dissociation of the ssRNA blocker and restoration of Cas12b activity during the subsequent temperature increase (Fig. 2d–f and Supplementary Fig. 3–5). Electrophoretic mobility shift assay results also revealed the ssRNA blocker markedly attenuated the formation of Cas12b/gRNA ribonucleoprotein (RNP) complexes and RNP-DNA complexes (Fig. 2g, h and Supplementary Fig. 6).

### TRACE assay analytical and clinical validation

We next performed a systematic optimization of the one-pot TRACE assay parameters. Comparable strong signal was detected in TRACE assays employing ssRNA blockers with annealing temperatures substantially less (–15 °C) than the Cas12b reaction temperature, whereas blockers with higher annealing temperatures resulted in attenuated signal (Supplementary Fig. 1e). More complex behavior was observed when ssRNA blocking sequence was appended to the gRNA sequence (Supplementary Fig. 1f), however, and such fusion gRNAs were therefore excluded from use in all subsequent studies, which employed ssRNA 1-S14. Subsequent optimization studies found that assays using a 1:4 gRNA:ssRNA blocker ratio, a poly T reporter, and 400 nM RNP yielded the best signal or signal-to-noise ratios when balancing cost and performance, and achieved a limit of detection (LoD) of 2.5 of *J2L* gene copies/test or 0.5 FFU/mL of viral particles when employing a 40-min protocol (10-min 37 °C and a 30-min 60 °C) (Fig. 3a, Supplementary Fig. 7 and S1g–j). This optimized TRACE assay revealed a broad

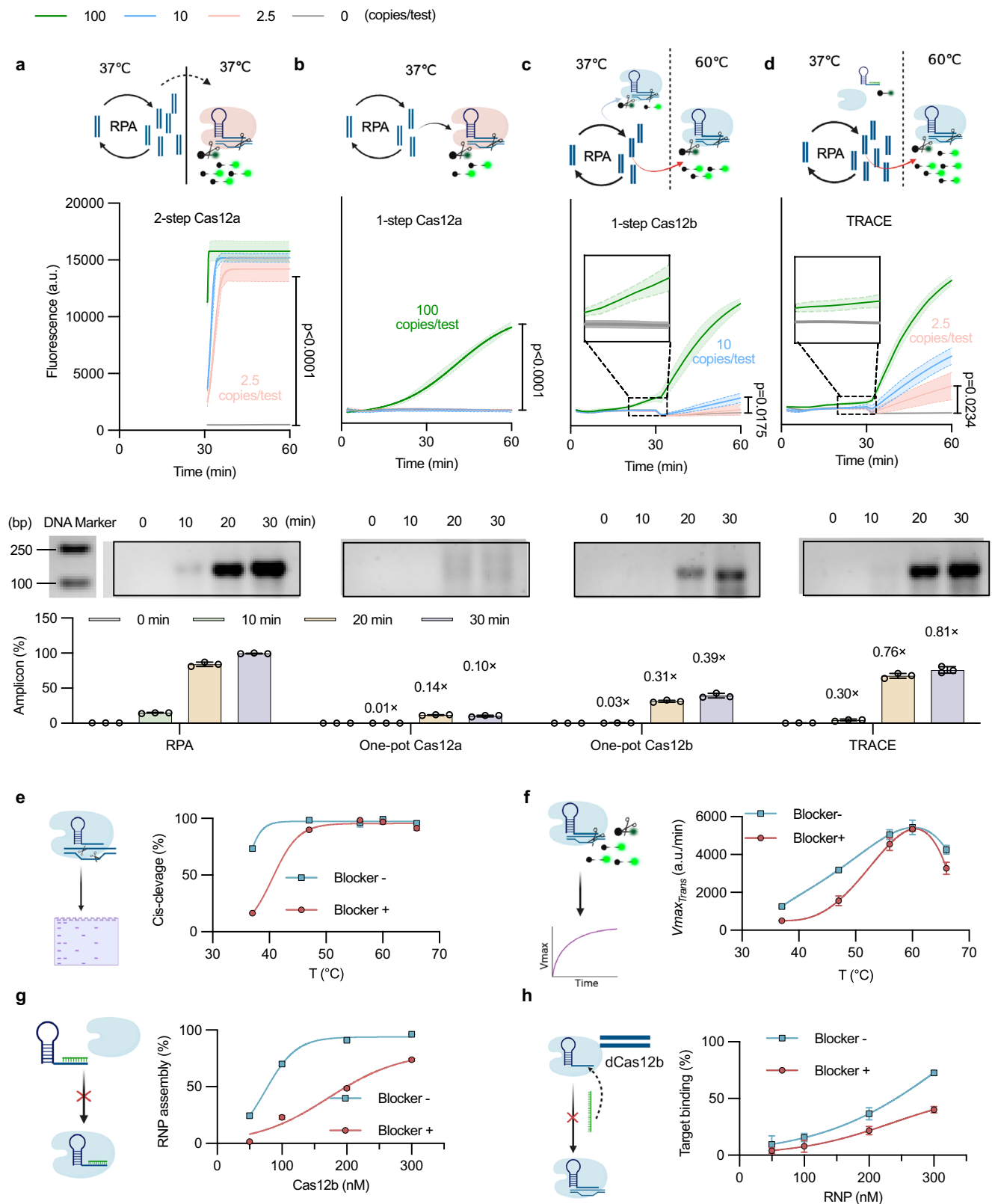
linear detection range (10–10,000 copies/test) and reliably detected MPXV DNA in at least 95% (19 of 20) of synthetic replicate samples at  $\geq 5$  copies/test sensitivity (Fig. 3b and Supplementary Fig. 8), without cross-reactivity with other orthopoxviruses or pathogens that can produce similar symptoms (Fig. 3c and Supplementary Table 3). TRACE also revealed compatibility with RPA analogs that employed different enzyme systems, including multienzyme isothermal rapid amplification and recombinase-aided amplification, and with divergent isothermal amplification systems such as rolling circle amplification (RCA) (Supplementary Fig. 9).

The diagnostic performance of this optimized TRACE assay (40-min protocol) was then evaluated using 118 qPCR-positive (Ct  $\leq 40$ ) biobank samples from 27 confirmed MPXV cases and 80 samples from 31 patients where MPXV infection was ruled out (Fig. 4 and Supplementary Table 4). Blinded analysis of nucleic acid extracts from these samples detected MPXV signal only in the samples obtained from MPXV patients, yielding sensitivity and specificity estimates of 99% (95% CI: 95–100) and 100% (95% CI: 96–100) and positive and negative predictive values of 100% (95% CI: 97–100) and 99% (95% CI: 92–100), misclassifying only one urine sample from an MPXV patient with a weakly positive qPCR result (Ct = 38) (Fig. 3d–e and Supplementary Fig. 10, and Supplementary Table 5). TRACE results also did not significantly differ when segregated by specimen type or the HIV status of the affected individuals (Fig. 3e, f), indicating their potential overall clinical utility.

Since assay performance time and sample throughput are often important criteria for diagnostics used to screen for emerging infectious diseases in clinical settings, we conducted a post-hoc analysis of the TRACE results for these clinical specimens to identify minimum time required to identify MPXV-infected individuals. Evaluation of the time-to-threshold (Tt) for positive signal in MPXV patient samples with a broad range of qPCR Ct values, revealed that 70% (83/118) of these samples achieved this threshold within 11 min (Fig. 3g), and all TRACE-positive samples had Tt values  $\leq 30$  min, indicating the potential to reduce the 2<sup>nd</sup> reaction stage time without compromising assay sensitivity. Subsequent analysis determined that an 18-min assay accurately identified 95% (95% CI, 89–98) of these sample, meeting a recently reported guideline for MPXV detection<sup>26</sup>, although specimen types that tend to have high viral loads, such as rash and saliva specimens, required less time (14 and 17 min) to achieve this classification accuracy (Fig. 3h and Supplementary Table 6). All subsequent assays were therefore performed using an 18-min TRACE protocol (10-min 37 °C and an 8-min 60 °C). Signals detected at this point revealed strong correlation ( $r = -0.8036$ ,  $p < 0.0001$ )<sup>27</sup> with qPCR results for samples with Ct values between 25–40 (Fig. 3i and Supplementary Fig. 11), suggesting the potential for semi-quantitative viral load estimation using TRACE results. Comparison of TRACE and qPCR results from two MPXV cases with serial rash or saliva specimens revealed corresponding trajectories for MPXV dynamics (Fig. 3j and Supplementary Fig. 12), suggesting the potential utility of TRACE results for rapid and robust tracking of MPXV viral load in these specimens.

### TRACE lateral flow assay design

MPXV infection are prevalent in resource-limited settings leading to an urgent need for diagnostics that can be employed in on-site screening efforts<sup>2,4</sup>. We therefore attempted to adapt TRACE to a point-of-care format by establishing a simple and streamlined workflow that integrates sample processing, analysis, and readout without requiring expensive equipment, and which employs lyophilized TRACE reagents that are stable at ambient temperature (Fig. 5a). Sample processing studies identified a 5-min temperature-agnostic MPXV lysis protocol that permitted efficient viral DNA release and detection when specimens were mixed with lysis buffer and then directly used as the input for a standard one-pot TRACE assay (Supplementary Fig. 13). Notably, this protocol performed well with samples that spanned



a wide range of pH values and  $\text{Na}^+$  concentrations and was compatible with diverse specimen types, including low viral titer plasma and urine samples, and these crude lysates yielded signal intensities and positivity rates comparable to those obtained with nucleic acid isolates from the corresponding specimens (Fig. 5b-c and Supplementary Fig. 14-16).

Lyophilization studies performed to eliminate cold-chain dependence, revealed that all five lyophilized reagent formulations produced signal comparable to native reagents (Fig. 5d and Supplementary Table 7). Stability testing of the reagents that produced the most consistent signal (formulation 4) revealed that that these reagents retained full activity for at least 60 days at 37°C (Fig. 5e), with

**Fig. 2 | Mechanistic of the TRACE assay.** **a–d** Signal dynamics of **(a)** two-step CRISPR/Cas12a, and one-pot **(b)** CRISPR/Cas12a, **(c)** CRISPR/Cas12b, and **(d)** TRACE assays when analyzing MPXV *J2L* gene standards (0–100 copies/test). Created in BioRender. Dong, Y. (<https://BioRender.com/931qrw6>). All assays used 400 nM RPA primers, 50 nM RNPs, and 500 nM reporter, while the TRACE assay also included 200 nM single-stranded RNA (ssRNA) blocker of the *J2L*-specific gRNA. Limits of detection (LoDs) were defined as the lowest *J2L* concentration yielding an endpoint signal significantly greater than the no-template control (NTC; 0 copy/test) background ( $\text{mean} + 3 \times \text{SD}$ ). Results are presented as the mean  $\pm$  SD (shaded region) of three technical replicates. *p* values were calculated using the two-tailed Wilcoxon signed-rank test relative to non-template control (NTC). *J2L* amplicon accumulation at designated time points in RPA and one-pot Cas12b, Cas12a, and TRACE assays, as indicated by representative PAGE images (top) and densitometry results (bottom) normalized to the mean of the 30-min RPA values. Numbers indicate the signal

detected vs. the corresponding RPA reaction time points. **e** Cas12b cis-cleavage efficiency and **(f)** trans-cleavage activity in CRISPR/Cas12b reactions performed at the indicated temperatures with and without a ssRNA gRNA blocker, as defined by **(e)** the decrease in dsDNA substrate PAGE band intensity after 2 min (Supplementary Fig. 2), and **(f)** the maximal trans-cleavage rate ( $V_{\text{max,trans}}$ ), as calculated from the first derivative of the fluorescence–time curve (Supplementary Fig. 3). **g, h** Electrophoretic mobility shift assays of **(g)** gRNA/Cas12b RNP and **(h)** RNP–DNA target complex formation at the indicated Cas12b and RNP concentrations with or without ssRNA gRNA blocker as defined by the decrease in intensity of the free gRNA and the free DNA bands (Supplementary Fig. 5). Created in BioRender. Dong, Y. (<https://BioRender.com/3fkvmok>). Data reflects mean  $\pm$  SDs values measured or derived from Image J analyses of three technical replicates. Source data are provided as a Source Data file.

estimated stabilities of > 4 months and 1.5 years without signal loss at 25 °C and 4 °C, respectively (Supplementary Table 8). Further, an optimized TRACE lateral flow assay (LFA) incorporating these lyophilized reagents revealed a LoD similar to the standard TRACE assay (10 vs. 2.5 copies/test), sufficient to distinguish MPXV-positive samples from non-MPXV samples (Fig. 5f, g and Supplementary Fig. 17–18). Together, these modular innovations enable TRACE to detect MPXV in clinical samples within 25 min, ~95 min faster than conventional qPCR assay (Fig. 5a and Supplementary Fig. 19).

### Retrospective and prospective evaluation of the TRACE LFA

We next performed a blinded analysis of 55 MPXV-positive and 47 MPXV-negative sample lysates (Fig. 4) using the TRACE fluorescent and LFA assay, and found the former accurately classified all samples whereas the latter returned false negatives for three MPXV-positive samples with Ct values > 33 (Fig. 6a, and Supplementary Fig. 20, and Supplementary Table 9). This streamlined TRACE LFA thus yielded sensitivity estimates of 86% (95% CI, 65–97) for samples with Ct values  $\geq$  31 when these samples were split into tertiles by their qPCR Ct results, and 95% (95% CI, 85–97) for all positive samples, whereas the fluorescent TRACE assay demonstrated a 100% (95% CI: 94–100) overall sensitivity estimate, and both assays exhibited 100% (95% CI: 92–100) specificity estimates.

Then, we conducted a prospective pilot study by integrating TRACE LFA into an outpatient workflow to facilitate rapid identification of suspected MPXV cases (Figs. 4, 6b and Supplementary Table 10). In this pilot study, rash swabs were sequentially collected from 28 symptomatic individuals with high epidemiological risk for MPXV infections, as determined by physician evaluation, and split for analysis with one of the two aliquots immediately tested on-site by TRACE LFA and the other transported to a central laboratory using a standard protocol and analyzed by a qPCR assay. TRACE LFA and qPCR results were fully concordant, correctly identifying all 11 MPXV and 17 non-MPXV cases (Fig. 6c and Supplementary Fig. 21). Notably, the mean sample-to-answer times of the TRACE LFA and qPCR were 30 min versus ~3 h in this study, indicating the potential feasibility of rapid on-site MPXV case identification by TRACE LFA results. TRACE LFA is also faster and more sensitive than most previously reported CRISPR-based MPXV assays and is - to the best of our knowledge - the only one supported by comprehensive clinical validation (Supplementary Table 11).

### Time resolution-based TRACE duplex assay

Since sampling defects can have strong detrimental effects on diagnostic test performance, as highlighted during the COVID-19 pandemic<sup>28</sup>, we next examined the potential to develop a duplex assay employing an internal control to identify potential false-negative results due to sample quality issues. Multiplex CRISPR assays are not normally feasible since Cas/gRNA complexes that recognize distinct

dsDNA sequences usually exhibit substantial cross-talk even when assays employ Cas variants with selective trans-cleavage sequence preferences<sup>21</sup>. However, we hypothesized that a Cas12a/gRNA RNP specific for a host gene could be incorporated into the RPA stage of TRACE so that the signals produced upon recognition of the host and pathogen target sequences could be distinguished by their detection interval. In this approach, Cas12a is active during the initial 37 °C assay stage but inactive during the subsequent 60 °C stage when Cas12b is active. Fluorescent signal increases detected during the first and second assay stages ( $\Delta F_1$  and  $\Delta F_2$ ) could thus be confidently attributed to the host gene internal control (e.g., RNase P gene) and the assay target (MPXV) to enable their dual detection in a single-reporter system (Fig. 7a).

We next optimized a duplex TRACE assay, which required increasing the second stage temperature from 60 °C to 64 °C to fully suppress Cas12a activity in the second stage and thus provide a stage-specific readouts for both targets (Fig. 7b, c and Supplementary Figs. 22, 23). Since competition between RPA and Cas12a activity during stage-1 (Fig. 2b) can adversely affect RNase P gene detection, both the stage-1 and stage-2 reactions employed a 30-min incubation to maximize the sensitive detection of both targets (Fig. 7a). This duplex assay revealed a 10 copies/test LoD for RNase P gene (Fig. 7d and Supplementary Fig. 24) and detected MPXV signal at 95% (19 of 20) of cell lysate samples spiked with a 10 copies/test *J2L* gene concentration (Fig. 7e and Supplementary Fig. 25). Subsequent analysis of 23 rash swabs from a small cohort of individuals with suspected MPXV infections (Fig. 4) detected RNase P gene signal in 22 of these 23 samples, and positive *J2L* signal in all 12 MPXV-positive samples, although this signal was very weak in the single RNase P-negative specimen, consistent with potential issues with the collection or preservation of this sample (Fig. 7f and Supplementary Fig. 26, 27).

Finally, to support future deployment of duplex TRACE diagnostics, we developed a small, inexpensive, and portable device that can perform and analyze TRACE duplex assays (Fig. 8a). This device employs an efficient thermal film to precisely control the assay temperature stages (Supplementary Fig. 28), and an optics design that uses a single excitation source and detector and can be powered by a rechargeable power-bank and controlled via a smartphone to allow real-time data acquisition and automated data analysis and interpretation in low-resource settings (Fig. 8b–e). TRACE duplex assay signals detected using a qPCR system and this device were highly similar and yielded concordant classifications when applied to analyze 23 biobank samples (Fig. 8f–g and Supplementary Fig. 29–30), and one sample was found to have invalid *J2L* and RNase P gene results indicative of a sample quality issue. A preliminary analysis also highlighted the cost advantage (\$3.8 vs. \$7.6/test) of deploying TRACE vs. qPCR, particularly in remote settings (Supplementary Figs. 31 and Supplementary Table 12).

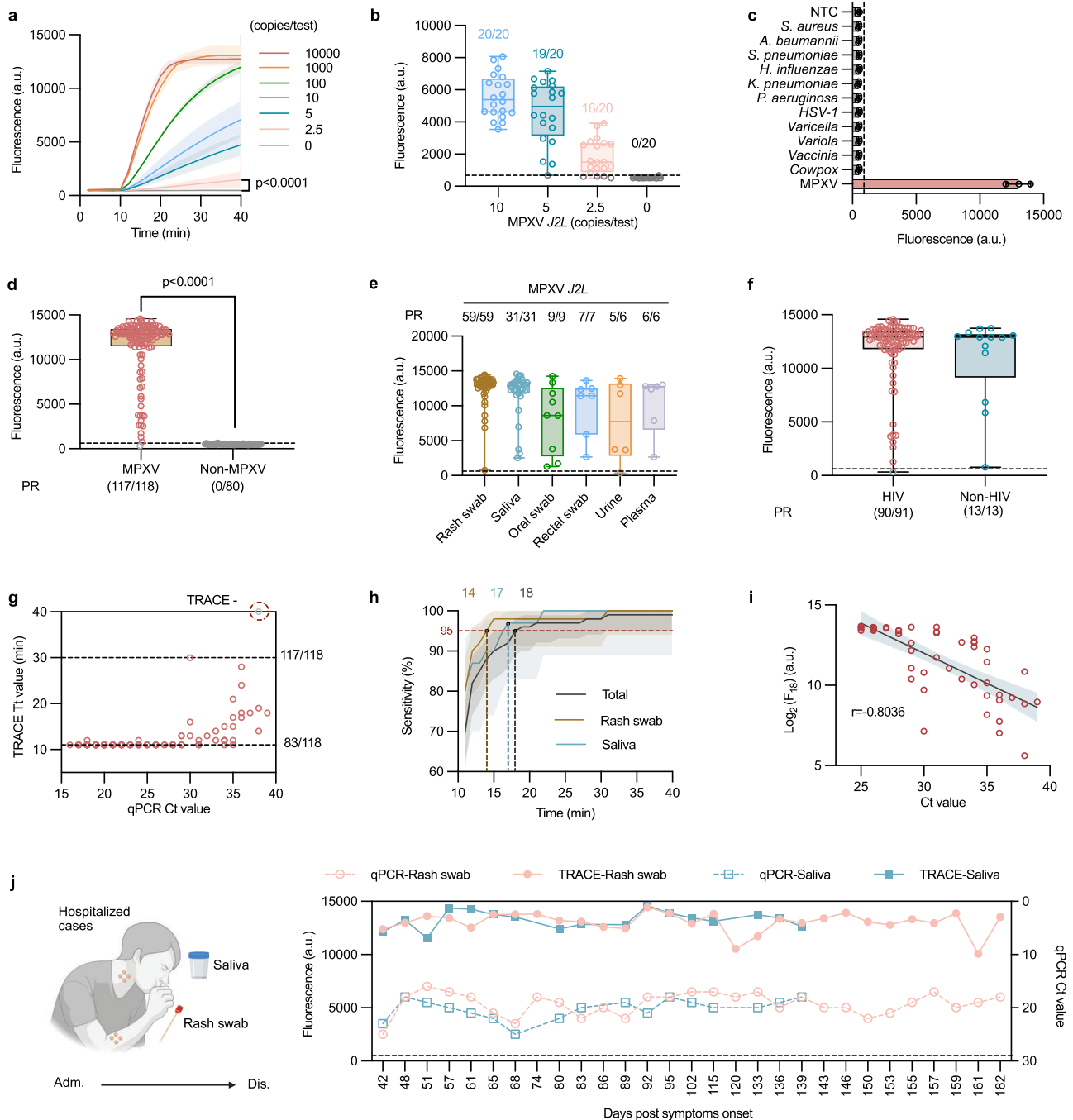


**Fig. 3 | Analytical and clinical characterization of the MPXV TRACE assay.**

**a** TRACE assay mean  $\pm$  SD (shadow) signal kinetics with serially diluted MPXV *J2L* gene standards ( $n = 3/\text{group}$ ).  $p$  values were calculated with two-tailed Wilcoxon signed-rank test to negative control. **b** TRACE reproducibility with replicate concentration standards (0 to 10 MPXV *J2L* gene copies/test;  $n = 20/\text{group}$ ). **c** TRACE MPXV specificity vs. other orthopoxviruses and related pathogens (mean  $\pm$  SD;  $n = 3/\text{group}$ ). **d** TRACE signals and positive rate (PR) detected in 118 MPXV-positive and 80 MPXV-negative samples. **(e)** in specific MPXV-positive sample types, and **(f)** in HIV infected and non-HIV infected MPXV cases. Fourteen samples from five individuals with undisclosed HIV status were excluded from the HIV subgroup analysis. **g** TRACE time-to-threshold (Tt) values vs. qPCR Ct values for the 118 MPXV-positive samples.

The false-negative urine sample was assigned a Tt value of 40 and marked by a dashed circle outline. **h** TRACE assay run time required to achieve 95% sensitivity in rash swab, saliva, and all specimen types. **i** Correlation between TRACE signal at 18 min ( $F_{18}$ ) and qPCR Ct value in MPXV-positive specimens with qPCR Ct values ranging from 25 to 40. **j** TRACE and qPCR results for serial rash swab and saliva specimens obtained from a representative MPXV case. Dashed lines indicate the thresholds for positive TRACE signal defined as the mean + 3 $\times$ SD of the NTC group (0 copy/test). Created in BioRender. Dong, Y. (<https://BioRender.com/falrvzxx>). In **b**, **e**, and **f**, box plots show median (centre line), interquartile range (box), whiskers indicating minima and maxima, with dashed lines marking cut-offs (also in **c**). In **h**, **i** shaded areas denote 95% CI. Source data are provided as a Source Data file.

**Discussion**

CRISPR-based assays offer a promising means to address diagnostic gaps, including the rapid response to emerging disease outbreaks<sup>29</sup>. However, their clinical translation is constrained by the challenge of developing one-pot and multiplex assays required for streamlined low

contamination risk workflows and quality control of diagnostic specimens<sup>9,10</sup>. Previous efforts have made limited progress in addressing these requirements<sup>9,14–23</sup>. However, our findings now indicate that one-pot duplex TRACE assays can detect a pathogen target (*J2L*) and host gene (RNase P) serving as an internal control for sample quality,

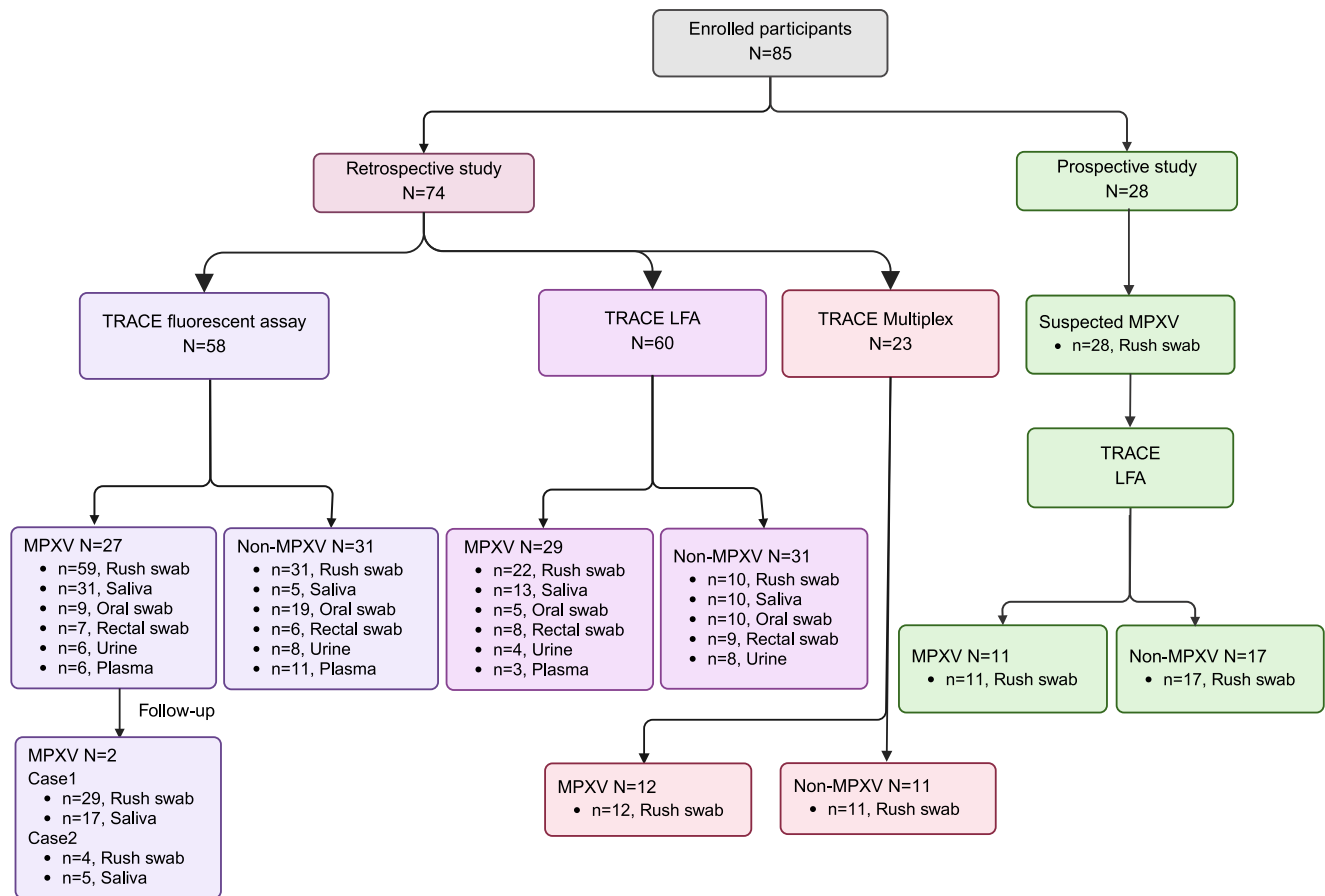


**Fig. 4 | Retrospective and prospective clinical cohort samples analyzed in this study.** Retrospective study samples were obtained from 74 participants diagnosed as MPXV or non-MPXV cases based on qPCR results. Remaining nucleic acid from the qPCR analysis and/or specimens were used for TRACE, TRACE LFA, and TRACE duplex analyses. Samples prospectively obtained from another

28 symptomatic individuals with epidemiological histories consistent with MPXV infection were analyzed in parallel by TRACE LFA (on-site) and qPCR (off-site central laboratory test). Created in BioRender. Dong, Y. (<https://BioRender.com/3n9e93c>).

and demonstrate strong diagnostic performance in clinical to point-of-care applications used to assess retrospective and prospective cohorts of clinical specimens (Supplementary Table 13).

Cas cis-cleavage activity in one-pot NAA/CRISPR assays is a recognized as a major limiting factor for their performance, since premature target amplicon degradation reduces NAA efficiency and the kinetics of the Cas trans-cleavage reaction that generates assay signal<sup>18,19,30</sup>. Current strategies have thus focused on attenuating Cas cis-cleavage activity in one-pot assays, by employing gRNAs that recognize sequences with suboptimal or missing protospacer adjacent motifs<sup>18,31</sup>, modified gRNAs that must be activated after NAA<sup>20,32</sup>, or chemicals that suppress Cas/gRNA complex formation and activity<sup>31</sup>. Reducing cis-cleavage activity to establish a more favorable balance between amplicon accumulation and consumption can improve the performance of one-pot CRISPR assays. However, NAA remains suboptimal for all these methods while attenuating Cas cis-cleavage also suppress its trans-cleavage activity, and both these issues act to limit the kinetics and sensitivity of the resulting assays. Such assays therefore continue to fall short of the performance of conventional two-step assays. Our basic one-pot TRACE assay format avoids these issues by using the temperature preferences of RPA and Cas12b—and a gRNA blocking sequence—to segregate its NAA and trans-cleavage reactions, each of which proceeds at its optimal temperature. The analytical sensitivity of this approach is comparable to two-step RPA/CRISPR assays<sup>33</sup>, and greater than reported for other one-pot CRISPR assays that detect MPXV. It should also represent a simpler, less expensive,

and more broadly applicable solution than reported gRNA photo-activation strategies used to induce Cas12a activity after completion of the NAA reaction. We observed that TRACE was compatible with diverse isothermal amplification methods, including two RPA analogs and rolling circle amplification. The enzymatic recombinase amplification (ERA), strand displacement amplification (SDA), and nucleic acid sequence-based amplification assays (NASBA) efficiently amplify target DNA within temperature ranges that are similar to RPA (37–42 °C), suggesting their potential utility in TRACE assays. However, TRACE assays employing alternate amplification may require optimization to attenuate buffer incompatibilities or other issues that could affect reliable assay performance.

Nonspecific Cas trans-cleavage activity has constrained the development of multiplex CRISPR assays<sup>9</sup>. The SHERLOCK V2 platform achieved four-plex detection by selecting Cas proteins with distinct substrate preferences<sup>21</sup>, but residual cross-reactivity between these systems can yield elevated backgrounds that undermine its specificity. Spatial separation strategies that analyze distinct CRISPR targets in reactions performed in distinct wells or channels of a microfluidic chip<sup>22,23,34</sup> are effective but require specialized equipment and expertise and have limited throughput, rendering them unsuitable to use in point-of-care applications. TRACE duplex assays leverage the distinct temperature optima and gRNA requirements of two Cas effector proteins, Cas12a and Cas12b, to resolve the signal produced upon recognition of distinct target amplicons during the two temperature stages of this assay. Reporter signal detected in the first assay stage

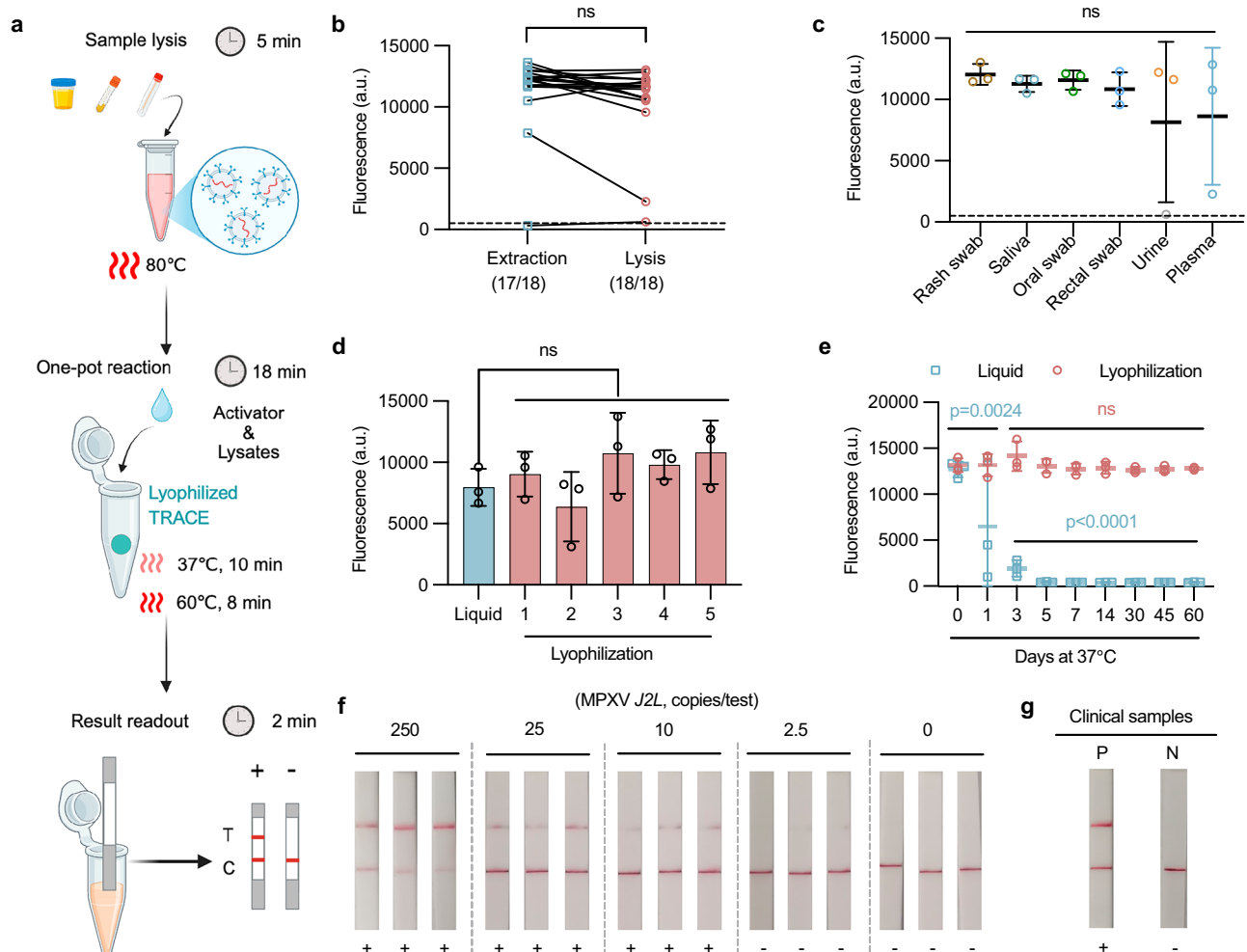


**Fig. 5 | TRACE lateral flow assay for MPXV point-of-care testing.** **a** Workflows of the 25-min TRACE LFA. Created in BioRender. Dong, Y. (<https://BioRender.com/a05xkfl>). **b, c** Comparison of TRACE signal detected with **(b)** lysates and DNA extracts of 18 clinical sample (rash, oral, and rectal swabs, saliva, urine, and plasma) from three MPXV patients, and **(c)** stratified by sample type. **d, e** Comparison of TRACE signal detected when samples containing **(d)** 25 MPXV *J2L* gene copies/test were analyzed by five lyophilized TRACE reagent formulations and the native TRACE reagents, or **(e)** 1000 MPXV *J2L* gene copies/test were analyzed by

lyophilized (formulation 4) and liquid TRACE reagents stored at 37 °C for the indicated times before use. **f, g** Images of TRACE LFA results detected for a series of **(f)** MPXV *J2L* gene standards ( $n = 3$  technical replicates per concentration), and **(g)** lysates of rash swab samples from a MPXV and a non-MPXV patient. Graphs **(c–e)** depict mean  $\pm$  SD values. Significant differences between groups were determined by **(b, c)** two-tailed Mann-Whitney test and **(d, e)** one-way ANOVA (ns,  $p > 0.05$ ). Source data are provided as a Source Data file.

exclusively reflects Cas12a recognition of its RNase P target since only this gRNA meets the Cas12a binding criteria and since interaction of the Cas12b-specific *J2L* gRNA with its ssDNA inhibitor attenuates Cas12b/gRNA formation and activity during this stage. Conversely, all reporter signal produced in the second stage reflects Cas12b recognition of its *J2L* target since Cas12a is immediately inactivated at the start of the second stage, so that only the newly formed *J2L*-specific Cas12b/gRNA complexes can produce target specific cleavage activity. This strategy effectively addresses a key limitation of most CRISPR assays, the absence of internal controls for specimen quality via concurrent detection of a host gene target. The use of a single reporter substantially simplifies the design of the portable reader for this assay and reduces its manufacturing cost. However, it may also be possible to adapt our current assay design to the general framework employed by the SHERLOCK V2 system to increase the multiplexing capacity of future TRACE assays, although this would require the discovery or engineering of new Cas variants that exhibit distinctive temperature preferences and trans-cleavage specificities.

This study has several limitations. First, further studies are required to fully characterize the behavior of lyophilized TRACE

reagents, particularly their long-term stability of under real-world storage and distribution conditions. Our results indicate that lyophilized TRACE reagents retain full activity for up to two months when stored at 37 °C, but more extreme and longer storage conditions should be investigated to better mimic those encountered in some resource limited regions. Second, our in-silico analyses suggest that our current assay should permit robust coverage of reported MPXV strains, but our validation studies were limited by the geographic homogeneity of sample collections sites, which are not expected to reflect the diversity MPXV strains now in circulation. Future studies should include MPXV lineages from a wider range of geographic sites where MPXV is endemic to evaluate the reliability of TRACE assay performance with genetically diverse strains. Fourth, diagnostic performance estimates for our TRACE assays should be validated in large, independent cohorts of distinct specimen types to confirm our findings. This is particularly important given that the post-hoc analysis we used to determine the time required achieve positive results was developed from a limited number of clinical specimens and could misrepresent the clinical diversity of this patient population. Nonetheless, our findings appear to constitute the largest and most

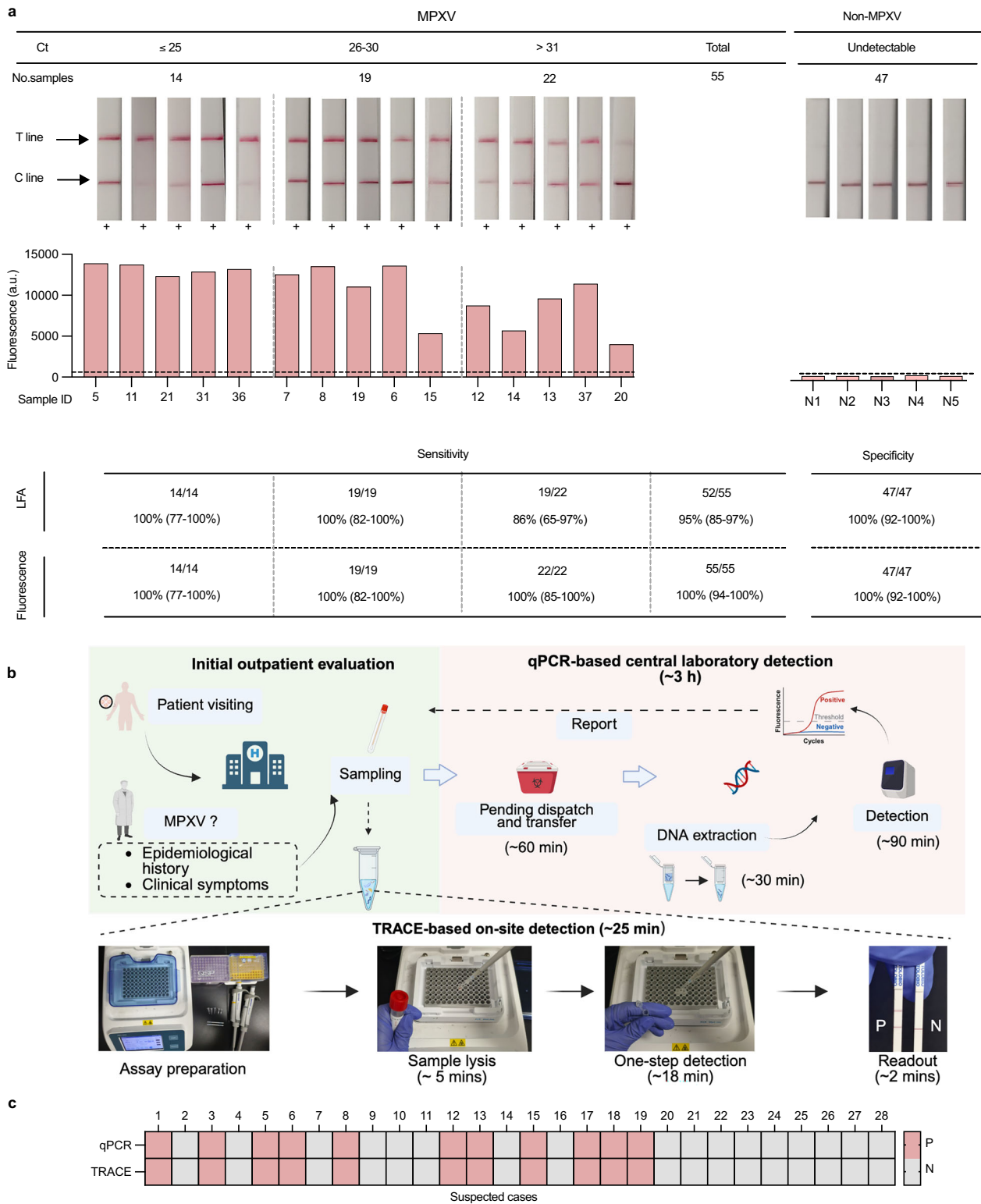


**Fig. 6 | TRACE LFA performance with retrospective and prospective MPXV cohorts. a** TRACE LFA and TRACE results of representative examples of 55 MPXV-positive and 47 MPXV-negative clinical samples stratified by their qPCR CT values and analyzed in parallel (complete results shown in Supplementary Fig. 20), and the sensitivity and specificity estimate of these Ct-stratified groups and the overall cohort. Graphed data depicts the results of

single assays performed with clinical samples. **b** Schematic of MPXV qPCR and TRACE LFA workflows in outpatient clinics. Created in BioRender. Dong, Y. (<https://BioRender.com/j2gxvri>). **c** TRACE LFA and central laboratory qPCR test results for 28 outpatients evaluated for suspected MPXV infections (details shown in Supplementary Fig. 21). Source data are provided as a Source Data file.

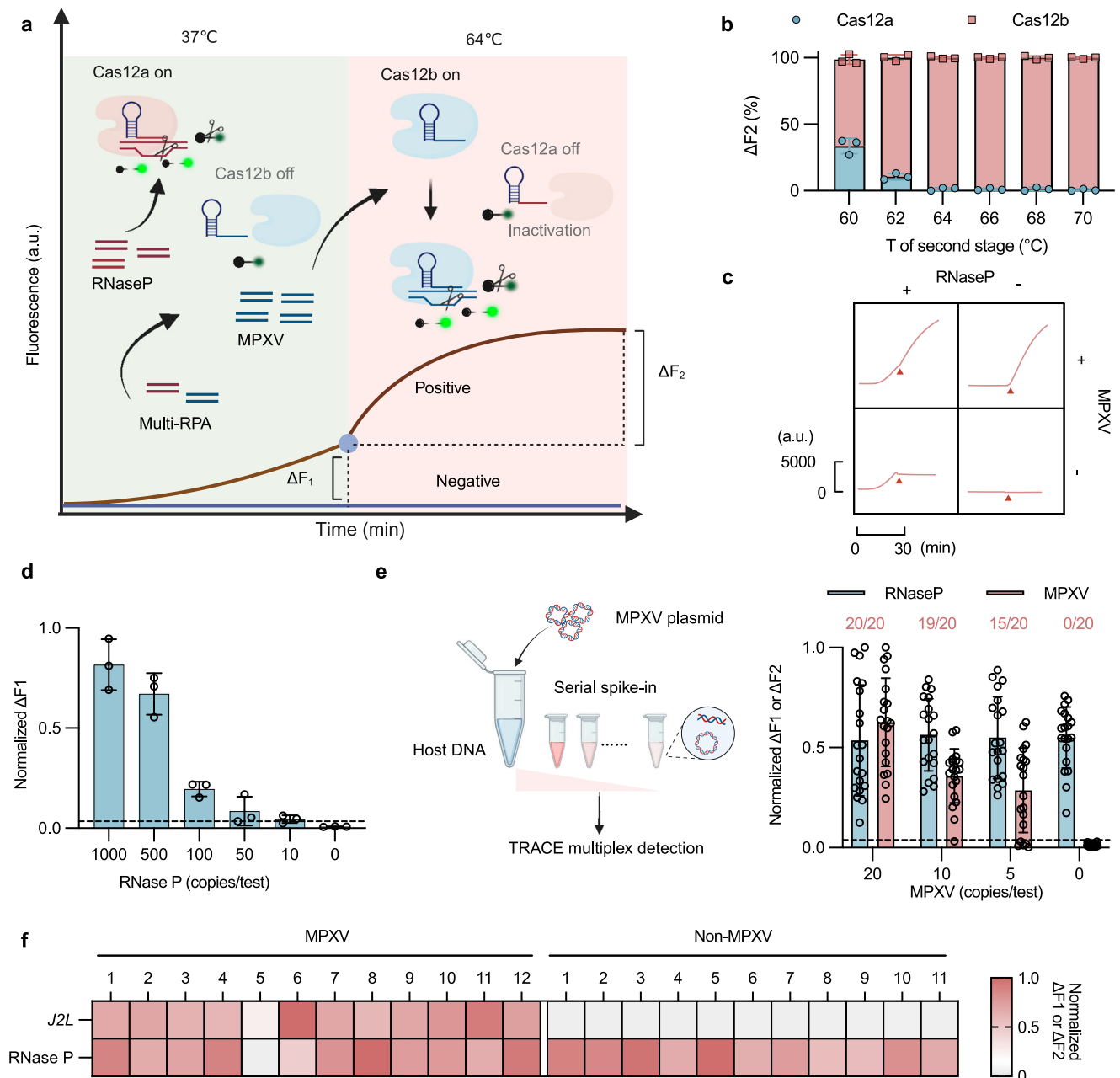


**Fig. 7 | TRACE duplex detection of MPXV and RNase P gene.** **a** Schematic of the TRACE duplex assay, indicating active duplex RPA reactions and CRISPR/Cas12a-mediated RNase P signal production in the 37 °C first stage, and subsequent RPA and Cas12a inactivation and formation of active Cas12b/gRNA complexes and MPXV *J2L* signal production upon release of the ssRNA blocker in the 64 °C second stage.  $\Delta F_1$  and  $\Delta F_2$  indicate host RNase P- and MPXV *J2L*-specific signals produced in the first and second stages, respectively. Created in BioRender. Dong, Y. (<https://BioRender.com/7yylkxh>). **b**  $\Delta F_2$  signal (%) contributed by Cas12a/gRNA and Cas12b/gRNA complexes at the indicated temperatures ( $n = 3$  samples/condition; detailed results shown in Supplementary Fig. 22). **c** Schematic of  $\Delta F_1$  and  $\Delta F_2$  signatures

characteristic of samples containing detectable levels of either, both, or neither of the RNase P (293 cell extracts) or MPXV *J2L* targets (100 copies/test). The red triangle denotes the point of temperature transition. **d** Normalized  $\Delta F_1$  signal detected for the indicated RNase P concentrations ( $n = 3$ /group). **e** Normalized  $\Delta F_1$  and  $\Delta F_2$  signal detected and target positivity rates in 293 cell nucleic acid extracts (103 ng/ $\mu$ L) spiked with the indicated MPXV *J2L* DNA concentrations. Created in BioRender. Dong, Y. (<https://BioRender.com/rwllkje>). **f** Normalized TRACE duplex assay RNase P  $\Delta F_1$  and MPXV *J2L*  $\Delta F_2$  signals detected in 12 MPXV-positive and 11 MPXV-negative clinical samples. Graphs indicate mean  $\pm$  SD values. Source data are provided as a Source Data file.

robust dataset employed to date to evaluate a CRISPR-based MPXV diagnostic assay (Supplementary Table 11). Finally, to minimize equipment costs, our portable detection device employed a simple fluorescence detection module and lacked an active cooling system, which limited its throughput and utility in real-world applications. Sensor optimization and noise reduction and other signal processing algorithms could be used to reduce signal variability in future devices,

and an active cooling system could be incorporated to extend the usable range of this device, as necessary.

TRACE meets “ASSURED” criteria for optimal point-of-care testing, which require assays to be Affordable, Sensitive, Specific, User-friendly, Rapid, Equipment-free, and Delivered. Specifically, TRACE’s \$3.8/test cost is approximately half qPCR’s, and should decrease with efficiencies of scale; has a 25-min sample-to-result workflow (vs. 3 h for

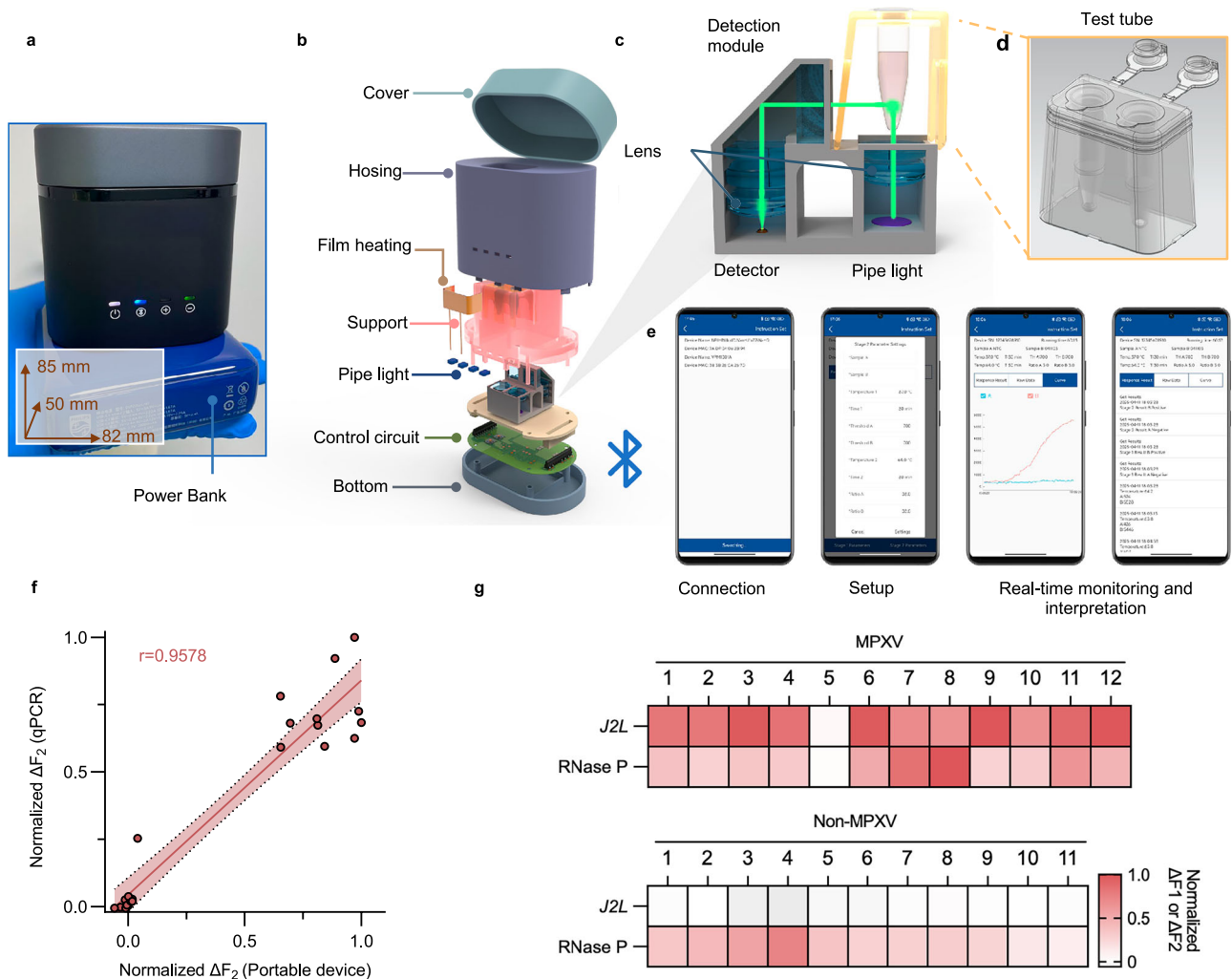


**Fig. 8 | TRACE duplex assay testing using a portable device suitable for on-site use.** **a** Photograph and **(b)** exploded schematic view of the internal architecture of this compact assay device, which employs a communication module for smartphone interaction and an external power bank to maximize operating time. The dimensions of the device are 82 mm × 50 mm × 85 mm (length × width × height). **c, d** Schematic of **(c)** the simplified optical system of this device that supports single-probe (FAM) detection from **(c)** dual detection ports to enable

simultaneous analysis of two samples. **(e)** Workflow indicating the smartphone-based assay setup, and real-time monitoring and interpretation of the assay results. **f** Correlation of TRACE *J2L*  $\Delta F_2$  signals detected with a qPCR system and the TRACE assay device using clinical samples (detailed results shown in Supplementary Fig. 29). **g** Normalized TRACE duplex assay RNase P  $\Delta F_1$  and MPXV *J2L*  $\Delta F_2$  signal of 12 MPXV-positive and 11 MPXV-negative clinical samples. Source data are provided as a Source Data file.

qPCR), while maintaining 99.5% diagnostic accuracy; employs simple equipment and lyophilized reagents suitable for use in resource-limited settings for on-site epidemic surveillance. Smartphone connectivity also enables real-time data analysis and reporting to facilitate epidemiology, public health responses, and telemedicine in under-served regions.

Our findings suggest that TRACE assays exhibit strong potential for clinical translation as duplex applications with internal quality control that should be suitable for rapid diagnosis of human pathogens using a variety of specimen types in an array of diagnostic settings, from clinical laboratories to resource-limited sites. Notably, both the benchtop and point-of-care TRACE assay formats sensitively detected MPXV in lysates of diverse patient specimen types, demonstrating strong concordance with qPCR results detected with nucleic acid extracts of these specimens. Further, when employed in a real-world outpatient setting, TRACE LFA demonstrated full agreement with qPCR while reducing diagnostic turnaround time by 83% to enable rapid on-site identification of MPXV cases and clinical decisions. We therefore propose that TRACE LFAs could provide a rapid, accurate,

and affordable diagnostic solution that could be deployed for use by individuals without significant technical expertise or additional equipment to overcome key barriers in translating CRISPR assays from bench to bedside.

## Methods

### Materials

The RPA Kit (25205), AapCas12b (32118), LbCas12a (32108), lateral flow strips (31203, lot 23114801), and sample lysis buffer [20 mM Tris-HCl (pH 8.0), 1% Tween-20, 1.5% NP-40, 0.02% SDS, 0.15 g/L PVP] were provided by Tolo Biotech (Shanghai, China). The Multienzyme Isothermal Rapid Amplification kit (WLB820IKIT), the Recombinase-aided amplification kit (B00000), and phi29 DNA Polymerase were purchased from Amp-Future Biotech (Weifang, China), Qitian Gene Biotech (Jiangsu, China), and Beyotime Biotech (Shanghai, China), respectively. T4 DNA ligase was purchased from NEB (Beijing, China). Oligonucleotides (Supplementary Data 2, Supplementary Table S1, and Supplementary Fig. 3) were synthesized by Sangon Biotech (Shanghai, China). The QIAamp DNA Mini Kit (51306) and the qPCR kit for MPXV

(AQ221-02) were obtained from QIAGEN (Shanghai, China) and TransGen Biotech (Beijing, China), respectively. dAapCas12b was prepared in-house. The HEK 293 cell strain (CRL-1573) was obtained from ATCC. Nucleic acids from pathogens used in the specificity assessment (Supplementary Table 3) were prepared in the BSL-3 laboratory at Shenzhen Third People's Hospital. All other chemical reagents were of analytical grade and purchased from Sigma-Aldrich.

### In silico analysis of primers and gRNA

An in-silico reference database was constructed (Supplementary Data 1)<sup>35</sup>, incorporating all available complete MPXV genomes ( $n = 2,525$ ) from the NCBI database, along with 304 randomly selected non-MPXV genomes, including orthopoxviruses, herpes simplex virus types 1 and 2, varicella-zoster virus, and other related viruses. Each primer and gRNA sequence were individually aligned to this database using the BLAST algorithm. As both RPA and CRISPR tolerate up to a single mismatch within primer or gRNA binding sites, alignment identity thresholds were adjusted accordingly. For each genome, three distinct elements, primer F and R and gRNA, had to meet the mismatch-tolerant alignment criteria. A genome was classified as a positive identification only if all three components simultaneously aligned within the permissible mismatch range. If any component failed to meet the criterion, the genome was considered “unmatched” and classified as TRACE-negative. These classification outcomes were then used to calculate the assay's overall sensitivity and specificity.

### Two-step CRISPR/Cas12a assay

The two-step assay involved distinct stages of RPA-based pre-amplification followed by CRISPR fluorescence detection, as follows: the lyophilized RPA pellets were resuspended in a reaction mixture containing 1  $\mu$ L of each forward and reverse primer (10  $\mu$ M) and 19.5  $\mu$ L of nuclease-free water. Subsequently, 1  $\mu$ L of activator and 2.5  $\mu$ L of target DNA at varying concentrations were added. The 25  $\mu$ L RPA reaction was incubated at 37 °C for 30 min. Then 2  $\mu$ L of the RPA product was transferred to a 20  $\mu$ L CRISPR reaction mixture containing a final concentration of 50 nM LbCas12a, 50 nM gRNA, and 500 nM fluorescent reporter. The fluorescence signal was monitored at 37 °C for 30 min and recorded every minute using the SLAN-96 real-time fluorescence detection system (HONGSHI, Shanghai).

### One-pot CRISPR/Cas12a or CRISPR/Cas12b assay

A master reaction mix was prepared containing final concentrations of 400 nM forward and reverse primers, 500 nM fluorescent reporter, 50 nM LbCas12a or AapCas12b, 50 nM gRNA, 1  $\mu$ L of activator, and 2.5  $\mu$ L of target DNA at varying concentrations, with the total reaction volume adjusted to 25  $\mu$ L using nuclease-free water. The master mix was incubated at 37 °C for 60 min for the CRISPR/Cas12a assay, and sequentially at 37 °C for 30 min followed by 60 °C for 30 min for the CRISPR/Cas12b assay. Fluorescence signals were recorded every minute.

### TRACE assay

The TRACE assay master mix was prepared with final concentrations of 400 nM forward and reverse RPA primers, 500 nM fluorescent reporter, 50 nM AapCas12b, 50 nM gRNA, and 200 nM ssRNA blocker. Additionally, 1  $\mu$ L of activator and 2.5  $\mu$ L of target DNA at varying concentrations were added, and the reaction volume was adjusted to 25  $\mu$ L with nuclease-free water. The reaction was carried out at 37 °C for 10 or 30 min, followed by 60 °C for 30 min. Fluorescence signals were measured every minute.

To optimize the performance of the TRACE assay, key components and reaction parameters of both the RPA and CRISPR systems were systematically adjusted, and the resulting maximum fluorescence signal was evaluated under each condition. Parameters optimized included primer and gRNA sequences (Supplementary Table 1), RPA

reaction time (0, 5, 10, 15, 20, or 30 min), RNP concentration (50, 100, 200, or 400 nM), and the gRNA-to-blocker ratio (1:1, 1:2, 1:4, 1:5, or 1:10).

### The amplicon accumulation evaluation of RPA and one-pot assays

The RPA master mixture contained 1  $\mu$ L each of forward and reverse primers (final concentration: 400 nM), 1  $\mu$ L of activator, and 2.5  $\mu$ L of *J2L* gene template (500 copies/test). One-pot CRISPR/Cas12a or Cas12b systems additionally included 50 nM gRNA and 50 nM Cas12a or Cas12b. For the TRACE system, 200 nM ssRNA blocker was further incorporated. All reactions were adjusted to a final volume of 25  $\mu$ L with nuclease-free water. Reactions were incubated at 37 °C for 0, 10, 20, and 30 min, and terminated at each time point with 0.1% SDS. Products were analyzed by 2% agarose gel electrophoresis, and band intensities were quantified using ImageJ ( $n = 3$ ). The 30-min RPA product served as a reference to calculate the percentage band intensity of each sample at different time points. Relative amplicon yield for the one-pot assays was calculated by dividing the mean band intensity of each system by that of RPA at the corresponding time point.

### Thermal dissociation dynamics of the ssRNA blocker

To form the quenched complex, 500 nM 3'-FAM-gRNA 1 and 2  $\mu$ M 5'-BHQ1-ssRNA blocker 1 were incubated at 70 °C for 5 min and then gradually cooled to room temperature to allow hybridization. The resulting 3'-FAM-gRNA/5'-BHQ1-blocker complex, along with individual controls (500 nM 3'-FAM-gRNA and 2  $\mu$ M 5'-BHQ1-blocker), was incubated at a series of constant temperatures (37 °C, 47 °C, 56 °C, 60 °C, and 66 °C), each for 2 min. Fluorescence signals were recorded every 30 seconds. Fluorescence recovery at each time point was calculated as the ratio of the fluorescence intensity of the 3'-FAM-gRNA/5'-BHQ1-blocker complex to that of free 3'-FAM-gRNA.

### Cis-cleavage activity of Cas12b with or without blocker

The gRNA or annealed gRNA-blocker (1:4) complex at 150 nM was first incubated with Cas12b (150 nM) at room temperature for 10 min. Subsequently, 14 nM of 5'-Cy5-labeled dsDNA substrate was added, and the reaction was carried out at various temperatures (37, 47, 56, 60, and 66 °C). Reactions were terminated at defined time points (0, 2, 5, 10, 15, 20, and 30 min) by adding 0.1% SDS. Reaction products were analyzed by 12% PAGE, and band intensities were quantified using Image Lab software (Bio-Rad, v6.1). Relative cis-cleavage activity was calculated as the percentage decrease in substrate band intensity at 2 min relative to that at 0 min.

### Trans-cleavage activity of Cas12b with or without blocker

The CRISPR master mix, comprising 50 nM AapCas12b, 50 nM gRNA or gRNA-blocker complex (1:4), 750 nM fluorescent reporter, and 14 nM dsDNA substrate, was incubated at 37 °C, 47 °C, 56 °C, 60 °C, or 66 °C for 20 min. Fluorescence signals were recorded at 1-min intervals, and the kinetic curve was generated by plotting fluorescence intensity over time. The slope of the curve at each time point was calculated, and the maximum slope observed during the reaction period was used to define the relative trans-cleavage activity.

### Expression and purification of dAapCas12b

The synthetic deactivated Cas12b (dCas12b) coding sequence carrying a single amino acid mutation (E848A) was cloned into a pET-based expression vector with a C-terminal 6 $\times$ His tag. Protein expression was induced in *Escherichia coli* strain BL21 ( $\Delta$ DE3) using 0.5 mM isopropyl- $\beta$ -D-thiogalactopyranoside at 16 °C for 16 h when the culture density reached an OD<sub>600</sub> of ~0.4. The induced cells were harvested, and cell pellets were lysed for protein purification. The supernatant of the lysate was incubated with His60 Ni resin (Takara) at 4 °C for 2 h, followed by elution with buffer (50 mM Tris-HCl, 1.0 M NaCl, 1 mM

dithiothreitol [DTT], 10 mM imidazole, and 5% glycerol, pH 8.0) containing increasing concentrations of imidazole (40, 60, 80, 100, 120, 150, and 200 mM). The eluted protein was subsequently concentrated using a 30 kDa centrifugal filter unit (Millipore) in elution buffer containing 50 mM Tris-HCl (pH 8.0), 400 mM NaCl, 2 mM DTT, and 0.2 mM ethylenediaminetetraacetic acid (EDTA). The final storage buffer consisted of 50 mM Tris-HCl (pH 8.0), 400 mM NaCl, 2 mM DTT, 0.2 mM EDTA, and 50% glycerol.

### EMAS evaluating AapCas12b binding affinity for gRNA with or without ssRNA blocker

Varying concentrations of AapCas12b (50, 100, 200, and 300 nM) were incubated with 50 nM of 5'-FAM-labeled gRNA or annealed 5'-FAM-labeled gRNA-blocker (1:4) mixture at 37 °C for 30 min to promote RNP formation. Then the reaction mixtures were analyzed on a 4% polyacrylamide gel, and band intensities of RNP complexes and free gRNA were quantified with Image Lab software. Binding efficiency was defined as the percent reduction in free gRNA band intensity, relative to the non-Cas12b control, across increasing concentrations of Cas12b.

### EMAS evaluating RNP binding affinity for dsDNA with or without ssRNA blocker

Varying concentrations of dCas12b/gRNA (1:1) RNP (50, 100, 200, and 300 nM) were incubated with 14 nM 5'-Cy5-labeled dsDNA with or without 200, 400, 800 nM and 1.2 μM ssRNA blocker, at 37 °C for 30 mins. Reaction mixtures were analyzed with a 4% polyacrylamide gel. Free dsDNA band intensities were quantified using Image Lab software. Binding affinity was defined as the percentage reduction in dsDNA fluorescence intensity relative to the non-dAapCas12b control across the concentration gradient.

### Lyophilization and long-term stability assessment of TRACE

To achieve optimal lyophilization performance for the TRACE assay, five different TRACE systems were formulated into a 20 μL master mix (Supplementary Table 7). The mixtures were then frozen at -50 °C for 1 h, followed by vacuum drying at -40 °C for 20 h to obtain lyophilized CRISPR pellets. For long-term stability assessment, the lyophilized CRISPR and RPA pellets were stored at 37 °C and tested at designated time points (0–60 days). As a control, the liquid TRACE was stored under identical conditions and subjected to head-to-head comparative testing. For performance evaluation, the lyophilized CRISPR and RPA pellets were resuspended in 21.5 μL of nuclease-free water, along with 1 μL activator and 2.5 μL target DNA. The reaction was incubated at 37 °C for 10 min, followed by incubation at 60 °C for 30 min. Fluorescence signals were recorded every minute.

### TRACE LFA assay

The TRACE LFA follows a similar workflow to the fluorescence-based TRACE assay but utilizes a colorimetric readout via lateral flow strips. Typically, 2.5 μL of target DNA was added to the master mix containing 400 nM forward and reverse primers, 20 nM FAM- and biotin-labeled reporter, 400 nM Cas12b, 400 nM gRNA, and 1.6 μM ssDNA blocker. The reaction was then carried out using the standard two-step temperature program of the TRACE assay. Following the reaction, 75 μL of TE buffer was added to dilute the reaction products and then test with a lateral flow strip by incubated at room temperature for 2–3 min before reading the results. Images of the test strips were captured, and the grayscale intensity of the T-line was quantified using ImageJ for semi-quantitative analysis. Optimum LFA reporter concentration was determined as the lowest reporter concentration (200, 100, 25, 10, 5, 2.5, and 0 nM) at which the FAM-specific gold nanoparticle-conjugated antibodies of the LFA produced staining only at the streptavidin-conjugated C-line of the LFA strip.

### Optimization of TRACE duplex assay

**Screening of RNase P gRNAs in the TRACE duplex assay.** TRACE duplex assay reactions were assembled using RNase P gRNA candidates (gRNA1–gRNA7). Each reaction was supplemented with 5 μL of nucleic acid extracts from human 293 cells and incubated at 37 °C for 30 min. Fluorescence signals were recorded every minute throughout the incubation.

**Optimization of RNP concentration for RNase P detection in the TRACE duplex assay.** TRACE duplex assay reactions were prepared using various concentrations (1000, 500, 250, 125 nM) of Cas12a–gRNA at a 1:1 molar ratio. Each reaction was supplemented with 5 μL of either human 293 cell nucleic acid extracts or nuclease-free water, followed by incubation at 37 °C for 30 min. Fluorescence signals were recorded every minute.

**Optimization of the second-phase temperature in the TRACE duplex assay.** Using the selected RNase P gRNA and optimized Cas12a/gRNA concentration, TRACE duplex reactions were assembled with 5 μL of either human 293 cell nucleic acid extracts or extracts spiked with 100 copies of the *J2L* gene. The reaction was first incubated at 37 °C for 30 min, followed by an additional 30-minute incubation at the indicated second-phase temperature (60–70 °C). Fluorescence signals were recorded every minute. The optimal second-phase temperature was defined as the condition under which the  $\Delta F_2$  signal from RNase P-only reactions was minimized, while the  $\Delta F_2$  signal from dual-target (RNase P + *J2L*) reactions was maximized, ensuring minimal interference from residual Cas12a activity.

### TRACE duplex assay

The optimized TRACE duplex assay was performed as follows: 400 nM of each primer for *J2L* and RNase P gene, 400 nM Cas12b, 500 nM Cas12a, 500 nM RNase P gRNA, 400 nM *J2L* gRNA, 500 nM fluorescent reporter, 1.6 μM ssRNA blocker, 1 μL activator, and 5 μL target DNA were combined into a 25 μL reaction system. The reaction was incubated at 37 °C for 30 min, followed by 64 °C for another 30 min. Fluorescence signals were recorded every minute using either a SLAN-96 real-time fluorescence detection system or a portable reader. Signals ( $\Delta F_1$ ) generated during the first 30 min were attributed to the RNase P gene, indicating acceptable clinical sample quality. Signal increases ( $\Delta F_2$ ) observed during the subsequent 30 min were attributed to the *J2L* gene, indicating the presence of MPXV.

To allow objective interpretation of duplex TRACE assay results, the change in stage-1 and stage-2 fluorescence signal ( $\Delta F_1$  and  $\Delta F_2$ ) of the negative control and MPXV negative samples were used to define the minimum thresholds for positive stage-1 and stage-2 signal ( $T_1$  and  $T_2$ ), which were defined as the mean + 3×SD values of the  $\Delta F_1$  and  $\Delta F_2$  values of the negative control and MPXV negative samples, respectively (Supplementary Fig. 27a). All analyzed samples with  $\Delta F_1$  and  $\Delta F_2$  values that exceed these  $T_1$  and  $T_2$  values are considered positive. Samples were considered RNase P-positive if  $\Delta F_1 > T_1$  and considered MPXV *J2L*-positive if  $\Delta F_2 > T_2$  regardless of their RNase P signal status. TRACE assay results for samples judged to be both RNase P-negative and *J2L*-negative were considered invalid.

### RCA-based TRACE assay

For a 20 μL ligation reaction, 5 μL of *J2L* (1000 copies per test) target with 3 μL padlock (10 μM) were first denatured at 95 °C for 5 min followed by 46 °C for 1 min before 2 μL T4 DNA ligase and 2 μL of T4 DNA ligase buffer were added. Ligation was performed at 37 °C for 1 h and then 80 °C for 5 min. Then 5 μL the ligation product was mixed with the 15 μL reaction system which contains 2 μL of phi29 buffer, 400 nM primer1, 1 μL of phi29 (10U/μL), 2 μL of dNTP (25 mM each), 1 μL of BSA (2 mg/mL), 400 nM Cas12b/gRNA RNP, 1.6 μM ssRNA blocker, and

500 nM reporter. The reaction was incubated at 30 °C for 60 min followed by 60 °C for 30 min.

### Analytical validation of the TRACE

**LoD.** A series of serially diluted target gene (*J2L* or RNase P) reference standards were analyzed under optimal assay conditions. The lowest concentration of the reference standard that generated a signal exceeding the positive threshold was defined as the LoD. The positive threshold was established as the mean signal value of the negative reference sample plus three times its standard deviation (SD).

**Analysis stability.** *J2L* gene reference standards at indicated concentrations were subjected to 20 repeated measurements. The lowest concentration with at least a 95% (19/20) detection probability across repeated tests was defined as the stable detection concentration.

**Analysis specificity.** Synthetic plasmids containing pathogen genes or extracted nucleic acids (Supplementary Table 3) from indicated pathogens were analyzed to assess cross-reactivity and assay specificity.

### Clinical validation of TRACE

**Clinical sample and information.** For the retrospective study, clinical samples, including rash fluid, oral and rectal swabs, saliva, blood, and urine, were collected from MPXV-infected and MPXV excluded cases admitted to Shenzhen Third People's Hospital between June 2023 and August 2024. Swab and saliva samples were stored in 3 mL of viral transport medium, while urine samples were aliquoted in sterile tubes. Blood samples were processed to separate plasma and stored in sterile tubes within 2 h of collection. All specimens were heat-inactivated at 56 °C for 30 minutes and stored at -80 °C until analysis. For the prospective study, suspected MPXV cases (a person with acute rash, fever > 38.5 °C, and lymphadenopathy, who within 21 days had traveled to a MPXV-endemic area, had close contact with a confirmed case, or was exposed to fluids from infected animals) were consecutively and indiscriminately enrolled at Shenzhen Third People's Hospital from December 2024 to April 2025, and available clinical specimens were collected.

**Clinical sample analysis.** All clinical samples were tested using qPCR in a clinical laboratory as a reference. Prior to qPCR analysis, nucleic acids were extracted from 200  $\mu$ L samples, yielding a final extraction volume of 50  $\mu$ L. Subsequently, 3  $\mu$ L of the extracted nucleic acids were analyzed using a commercial qPCR kit. Samples with a Ct value below 40 were classified as positive, with the Ct value reported as a reference for semi-quantitative analysis, while samples with a Ct value of 40 or higher were considered negative.

All nucleic acid samples were blindly tested using the TRACE assay with 1  $\mu$ L of extracted nucleic acid. To assess the performance of the TRACE LFA, original clinical samples were mixed directly with sample lysis buffer at a 3:1 ratio and incubated at 80 °C for 5 min to facilitate lysis. Subsequently, 5  $\mu$ L of the lysate, 1  $\mu$ L of activator and 19  $\mu$ L of nuclease-free water were added to the lyophilized TRACE or the TRACE duplex system, gently mixed, and run the detection with the pre-defined temperature program. The results were obtained by measuring fluorescence signals using the SLAN-96 real-time fluorescence detection system or by visual interpretation using LFA strips.

### Statistics & reproducibility

The sample size for clinical validation was calculated according to previous reports<sup>30,33</sup>, the target sensitivity and specificity for the TRACE were set at 90% and 95%, respectively, with expected sensitivity and specificity of 98% and 100%. Assuming a two-sided  $\alpha$  of 0.05 and  $\beta$  of 0.2, a minimum of 78 positive samples and 73 negative samples were required to meet statistical requirements. Laboratory personnel

responsible for sample testing were blinded to the clinical classification data until the analysis stage. No data were excluded from the analysis.

Experimental results are reported as mean  $\pm$  standard deviation (SD) values. Participant characteristics were summarized using medians, interquartile ranges, and proportions. Differences in TRACE signals across groups were analyzed using the Mann–Whitney U test, Wilcoxon signed-rank test, or repeated-measures one-way/two-way ANOVA ( $\alpha = 0.05$ ), as indicated in the figure legends. Spearman's correlation analysis was performed to evaluate the agreement between TRACE and qPCR results, as well as between extracted and unextracted samples. Sensitivity and specificity were calculated with exact 95% confidence intervals based on a binomial distribution, and accuracy, positive and negative predictive value were estimated. The gel band intensities were analyzed using Image Lab software (Bio-Rad, v6.1) and lateral flow test strip signals were quantified with NIH ImageJ software (v1.54.J). Statistical analyses and data visualization were performed using GraphPad Prism (v10.4.1).

### Ethical statement

All Clinical samples and de-identified clinical information were collected after obtaining prior written informed consent from participants, with IRB protocols approved by the Ethical Review Board of the Third People's Hospital of Shenzhen (2023-006-02, 2023-051, and 2024-005). The de-identified clinical data, including demographic information and laboratory test results, were collected from the electronic medical records system according to ethical guidelines.

### Reporting summary

Further information on research design is available in the Nature Portfolio Reporting Summary linked to this article.

### Data availability

All data generated in this study are provided in the Supplementary Information and Source Data within this paper. Source data are provided with this paper.

### Code availability

The code for in-silico analysis of the primers and gRNAs is available at the GitHub repository: <https://github.com/MangoBank/InSiliconAnalysis> and Zenodo<sup>35</sup>.

### References

1. Organization, W. H. Pathogens prioritization: a scientific framework for epidemic and pandemic research preparedness. *World Health Organization: Geneva, Switzerland* (2024).
2. Mitjà, O. et al. Monkeypox. *Lancet* **401**, 60–74 (2023).
3. Organization, W. H. in *Global Mpox Trends Global Mpox Trends* (ed World Health Organization) (World Health Organization, 2025).
4. Brosius, I. et al. Epidemiological and clinical features of mpox during the clade Ib outbreak in South Kivu, Democratic Republic of the Congo: a prospective cohort study. *Lancet* **405**, 547–559 (2025).
5. Lee, B. U. Airborne transmission of MPXV and its aerosol dynamics under different viral load conditions. *Lancet Microbe* **4**, e288–e289 (2023).
6. Ndembi, N. et al. Evolving epidemiology of Mpox in Africa in 2024. *N. Engl. J. Med.* **392**, 666–676 (2025).
7. Solomon Abebe, Y. et al. Rapid diagnostic test: a critical need for outbreak preparedness and response for high priority pathogens. *BMJ Glob. Health* **9**, e014386 (2024).
8. Land, K. J., Boeras, D. I., Chen, X.-S., Ramsay, A. R. & Peeling, R. W. REASSURED diagnostics to inform disease control strategies, strengthen health systems and improve patient outcomes. *Nat. Microbiol.* **4**, 46–54 (2019).
9. Huang, Z., Lyon, C. J., Wang, J., Lu, S. & Hu, T. Y. CRISPR assays for disease diagnosis: progress to and barriers remaining for clinical applications. *Adv. Sci.* **10**, 2301697 (2023).

10. Kaminski, M. M., Abudayyeh, O. O., Gootenberg, J. S., Zhang, F. & Collins, J. J. CRISPR-based diagnostics. *Nat. Biomed. Eng.* **5**, 643–656 (2021).
11. Chen, J. et al. CRISPR-Cas12a target binding unleashes indiscriminate single-stranded DNase activity. *Science* **360**, 436–439 (2018).
12. Gootenberg, J. S. et al. Nucleic acid detection with CRISPR-Cas13a/C2c2. *Science* **356**, 438–442 (2017).
13. Li, S. Y. et al. CRISPR-Cas12a-assisted nucleic acid detection. *Cell Discov.* **4**, 20 (2018).
14. Wang, B. et al. Cas12aVDet: a CRISPR/Cas12a-based platform for rapid and visual nucleic acid detection. *Anal. Chem.* **91**, 12156–12161 (2019).
15. Chen, Y. et al. Contamination-free visual detection of SARS-CoV-2 with CRISPR/Cas12a: a promising method in the point-of-care detection. *Biosens. Bioelectron.* **169**, 112642 (2020).
16. Joung, J. et al. Detection of SARS-CoV-2 with SHERLOCK One-Pot Testing. *N. Engl. J. Med.* **383**, 1492–1494 (2020).
17. Arizti-Sanz, J. et al. Streamlined inactivation, amplification, and Cas13-based detection of SARS-CoV-2. *Nat. Commun.* **11**, 5921 (2020).
18. Lu, S. et al. Fast and sensitive detection of SARS-CoV-2 RNA using suboptimal protospacer adjacent motifs for Cas12a. *Nat. Biomed. Eng.* **6**, 286–297 (2022).
19. Tong, X. et al. Fast and sensitive CRISPR detection by minimized interference of target amplification. *Nat. Chem. Biol.* **20**, 885–893 (2024).
20. Hu, M. et al. Photocontrolled crRNA activation enables robust CRISPR-Cas12a diagnostics. *Proc. Natl. Acad. Sci.* **119**, e2202034119 (2022).
21. Gootenberg, J. S. et al. Multiplexed and portable nucleic acid detection platform with Cas13, Cas12a, and Csm6. *Science* **360**, 439–444 (2018).
22. Ackerman, C. M. et al. Massively multiplexed nucleic acid detection with Cas13. *Nature* **582**, 277–282 (2020).
23. Welch, N. L. et al. Multiplexed CRISPR-based microfluidic platform for clinical testing of respiratory viruses and identification of SARS-CoV-2 variants. *Nat. Med.* **28**, 1083–1094 (2022).
24. Yang, Y. et al. Longitudinal viral shedding and antibody response characteristics of men with acute infection of monkeypox virus: a prospective cohort study. *Nat. Commun.* **15**, 4488 (2024).
25. Teng, F. et al. Repurposing CRISPR-Cas12b for mammalian genome engineering. *Cell Discov.* **4**, 63 (2018).
26. Center, C. N. M. P. A. *Guidelines for Registration and Review of Poxvirus Nucleic Acid Detection Reagents* (China National Medical Products Administration Center, 2023).
27. Schober, P., Boer, C. & Schwarte, L. A. Correlation coefficients: appropriate use and interpretation. *Anesthesia & Analgesia* **126**, 1763–1768 (2018).
28. Kinloch, N. N. et al. Suboptimal biological sampling as a probable cause of false-negative COVID-19 diagnostic test results. *J. Infect. Dis.* **222**, 899–902 (2020).
29. Fleming, K. A. et al. The Lancet Commission on diagnostics: transforming access to diagnostics. *Lancet* **398**, 1997–2050 (2021).
30. Wang, Y. et al. Ultrasensitive single-step CRISPR detection of monkeypox virus in minutes with a vest-pocket diagnostic device. *Nat. Commun.* **15**, 3279 (2024).
31. Cheng, Z.-H. et al. Tunable control of Cas12 activity promotes universal and fast one-pot nucleic acid detection. *Nat. Commun.* **16**, 1166 (2025).
32. Liu, P. et al. Universal crRNA acylation strategy for robust photo-initiated one-pot CRISPR-Cas12a nucleic acid diagnostics. *Angew. Chem. Int. Ed.* **63**, e202401486 (2024).
33. Low, S. J. et al. Rapid detection of monkeypox virus using a CRISPR-Cas12a mediated assay: a laboratory validation and evaluation study. *Lancet Microbe* **4**, e800–e810 (2023).
34. Lamb, C. H., Kang, B. & Myhrvold, C. Multiplexed CRISPR-based Methods for Pathogen Nucleic Acid Detection. *Curr Opin Biomed Eng* **27**, 100471 (2023).
35. Huang, Z. et al. Thermally programmed one-pot CRISPR assay for on-site pandemic surveillance. *InSiliconAnalysis*, <https://doi.org/10.5281/zenodo.17187568> (2025).

## Acknowledgements

The work was supported by the National Natural and Science Foundation of China (82302614 to Z.H., 31922046 to J.W.), the “Leading Goose” R&D Program of Zhejiang (2023C03045 to G.P.Z.), the Medical Scientific Research Foundation of Guangdong Province (A2023170 to Z.H.), the Guangdong Basic and Applied Basic Research Foundation (2025A1515011871 to Z.H.).

## Author contributions

Z.H. and J.W. conceived the project and designed the experiments. Y.J.D., X.C.H., S.D. and C.H. conducted the major experiments. Z.H., Y.J.D., X.C.H., Y.Y., G.G.Z. and H.H. contributed to the data analysis and interpretation. Y.Y., Y.P., F.X.W. and L.Y. contributed to the clinical information and sample collection and analysis. Z.H. drafted the manuscript. C.J.L., G.P.Z., X.Y.F., S.H.L., T.H. and J.W. provided critical revision. All the authors approved the final manuscript and J.W. was responsible for the decision to submit the manuscript. We gratefully acknowledge DIAN Diagnostics for their generous contribution of qPCR reagents.

## Competing interests

X.H., S.D. and J.W. are ToloBio employees and G.P.Z. and J.W. are cofounders of ToloBio. All other authors declare no competing interests.

## Additional information

**Supplementary information** The online version contains supplementary material available at <https://doi.org/10.1038/s41467-025-65193-1>.

**Correspondence** and requests for materials should be addressed to Xiao-Yong Fan, Shuihua Lu, Tony Hu or Jin Wang.

**Peer review information** *Nature Communications* thanks Zhen Rong, and the other, anonymous, reviewer(s) for their contribution to the peer review of this work. A peer review file is available.

**Reprints and permissions information** is available at <http://www.nature.com/reprints>

**Publisher’s note** Springer Nature remains neutral with regard to jurisdictional claims in published maps and institutional affiliations.

**Open Access** This article is licensed under a Creative Commons Attribution-NonCommercial-NoDerivatives 4.0 International License, which permits any non-commercial use, sharing, distribution and reproduction in any medium or format, as long as you give appropriate credit to the original author(s) and the source, provide a link to the Creative Commons licence, and indicate if you modified the licensed material. You do not have permission under this licence to share adapted material derived from this article or parts of it. The images or other third party material in this article are included in the article’s Creative Commons licence, unless indicated otherwise in a credit line to the material. If material is not included in the article’s Creative Commons licence and your intended use is not permitted by statutory regulation or exceeds the permitted use, you will need to obtain permission directly from the copyright holder. To view a copy of this licence, visit <http://creativecommons.org/licenses/by-nc-nd/4.0/>.

© The Author(s) 2025